

Chaotic instability in the BFSS matrix model

Osamu Fukushima^{‡*} and Kentaroh Yoshida^{‡†}

[‡]*Department of Physics, Kyoto University, Kyoto 606-8502, Japan.*

Abstract

Chaotic scattering is a manifestation of transient chaos realized by the scattering with non-integrable potential. When the initial position is taken in the potential, a particle initially exhibits chaotic motion, but escapes outside after a certain period of time. The time to stay inside the potential can be seen as lifetime and this escape process may be regarded as a kind of instability. The process of this type exists in the Banks-Fischler-Shenker-Susskind (BFSS) matrix model in which the potential has flat directions. We discuss this chaotic instability by reducing the system with an ansatz to a simple dynamical system and present the associated fractal structure. We also show the singular behavior of the time delay function and compute the fractal dimension. This chaotic instability is the basic mechanism by which membranes are unstable, which is also common to supermembranes at quantum level.

*E-mail: osamu.f@gauge.scphys.kyoto-u.ac.jp

†E-mail: kyoshida@gauge.scphys.kyoto-u.ac.jp

Contents

1	Introduction	1
2	An overview of chaotic scattering	3
3	Chaotic scattering in a four-hill potential model	5
3.1	Four-hill potential model	5
3.2	Self-similarity in the initial points	5
3.3	Time delay function	8
4	Chaotic instability in the BFSS matrix model	10
5	Conclusion and Discussion	14

1 Introduction

Chaos is a significant characteristic of nonlinear dynamics. Classically chaotic systems exhibit highly complex trajectories and the dynamics cannot be solved analytically. The complexity can be measured by positive Lyapunov exponents and non-quasiperiodic plots in Poincaré section. Recently, there has been an attempt to figure out chaotic behavior in the scattering process [1–3]. The S-matrix, which is one of the most important physical quantities, is a good target to tackle chaotic behavior in the context of field theory. In fact, chaotic behavior in the scattering process of non-integrable dynamical systems has long been well studied. This is called “*chaotic scattering*”.

What is the difference between the usual classical chaos and chaotic scattering? Classical chaos is usually characterized by long-time behavior. Therefore, we need to confine the system or consider an energy region where all motions are restricted to a finite region. However, there is another kind of chaos which appears for finite time. This is called transient chaos. It may sound like a recurrence, but chaotic behavior can be clearly distinguished, for example, by making sure that the spectrum is continuous. Chaotic scattering is a manifestation of this transient chaos.

How can one see this transient chaos? Let us consider a non-integrable system with a finite scattering region. Then a finite-time chaotic behavior is observed during a particle is passing through (or staying in) the scattering region, while the particle is free outside the scattering region. This is nothing but the transient chaos that is identified as the chaotic

scattering. This chaotic scattering has been investigated in various models such as the Hénon-Heiles system and the Contopoulos system. It also shows stretching and folding of the phase space and consequently leads to a horse-shoe construction of stable manifolds. This indicates that the chaotic scattering should also have a fractal structure.

It is well known that classical Yang-Mills theory exhibits classical chaos [4]. Similarly, the Banks-Fischler-Shenker-Susskind (BFSS) matrix model [5], which is a one-dimensional matrix quantum mechanics, is also chaotic [6]¹. The BFSS matrix model is a matrix realization of light-front M-theory and a matrix regularization of the supermembrane theory [9]. The potential of the BFSS matrix model has flat directions and a motion along this direction may escape from the chaotic region to a spatial infinity. Hence the BFSS matrix model may exhibit transient chaos. These flat directions are considered as the origin by which supermembranes are unstable at quantum level [10].

In this paper, we discuss chaotic scattering in the context of the BFSS matrix model. By reducing the model to a simple dynamical system with a specific ansatz, we study the fuzzy membrane dynamics. The initial configuration initially moves in the chaotic region of the potential, but extends infinitely long along a flat direction after a certain period of time. This infinitely long extension, which indicates membrane instability [10], corresponds to the escape process in chaotic scattering. Once this instability is recognized as a chaotic scattering process, we can present the associated fractal structure and compute the life time of the configuration. The singularities in the time delay function form a Cantor-like set and its fractal dimension can be estimated by means of uncertain fraction. Thus a fractal structure behind the BFSS matrix model is unveiled by reformulating the membrane instability [10] as a chaotic scattering process.

This paper is organized as follows. Section 2 provides an overview of chaotic scattering. In Section 3 we consider a system with a four-hill potential as a concrete example. A fractal structure appears in the space of initial conditions for which trajectories survive at a certain time t . The singularities in the time delay function forms a Cantor-like set with a fractal dimension. In Section 4, by reducing the BFSS matrix model to a simple dynamical system, the membrane instability is reinterpreted as the chaotic scattering. The analysis is almost parallel to the four-hill case. Section 5 is devoted to conclusion and discussion.

¹The Berenstein-Maldacena-Nastase (BMN) matrix model [7], which is a kind of massive deformation of the BFSS matrix model, also shows classical chaos [8]. In this case, the flat directions in the BFSS matrix model are lifted up by mass terms and thus all of the classical motions are completely bounded.

2 An overview of chaotic scattering

Let us here give an overview of chaotic scattering in a general setup. For good reviews, for example, see [11, 12]. Some of the results in [11] are reproduced by our own program.

General characteristics of classical chaos

Classical chaos is usually discussed in a bounded system in order to study long-time behaviors of trajectories. A chaotic dynamical system has the following two characteristics:

1. strong sensitivity to initial conditions,
2. fractal from a symbolic dynamics.

The first property can be measured by the Lyapunov spectrum. Suppose that a solution $\mathbf{x}(t)$ is chaotic and consider a nearby point $\mathbf{x}(t) + \delta\mathbf{x}(t)$. Then the deviation $\delta\mathbf{x}(t)$ grows exponentially like

$$|\delta\mathbf{x}(t)| \sim |\delta\mathbf{x}(0)| e^{\lambda t}. \quad (2.1)$$

The constant parameter λ is a Lyapunov exponent. This means that tiny differences in the initial conditions will grow exponentially over time. This property is often called the butterfly effect.

The second means that a fractal structure exists behind classical chaos and this fractal arises from a symbolic dynamics generated by chaotic trajectories. Then the trajectories give rise to a Smale horseshoe. The horseshoe construction leads to fractal structures.

Chaotic scattering as transient chaos

Transient chaos is a phenomenon where a system exhibits chaos over *finite* time, while traditional chaos is rather characterized by a *long*-time behavior. When a non-integrable system is defined in an asymptotically flat space and has a finite scattering region, a finite-time chaotic behavior is observed during a particle is passing through (or staying in) the scattering region, while the particle is free outside the scattering region. This is an example of transient chaos that is identified as the *chaotic scattering*.

In comparison to the usual chaos, it is not so suitable to study the Lyapunov exponent because a particle will escape from the scattering region. However, this escape process is a characteristics of chaotic scattering and one can consider other quantities. For example,

when one sees the space of initial conditions for which trajectories remain in the scattering region, there exist some gaps which corresponds to escaped trajectories. Then the gaps define topology. The number of gaps increases exponentially over time like

$$N(t) \sim N(0) e^{ht}. \quad (2.2)$$

Here h is referred to as the topological entropy because the escaped trajectories imply the information loss.

In addition, the gaps show a self-similar structure, which is nothing but fractal. Note here that this is concerned with the escape process and is different from the fractal associated with classical chaos in a bounded system. In this paper we are concerned with this fractal associated with the escape process.

There are two kinds of setup to study chaotic scattering.

1. *Scattering* One can study literally scattering process when the potential is asymptotically flat. A particle comes from spatial infinity and enter into the scattering region. Then it stays there for a while and exhibits classical chaos. Finally, it escapes from the scattering region and go off to spatial infinity. The scattering angle as a function of impact parameter is a representative physical quantity in this setup. For more detailed discussions, see e.g. [11].
2. *Decay* Instead of considering an in-coming particle, it is also possible to take the initial condition in the scattering region. Then the particle initially exhibits chaotic motion and then escapes from there after a certain period of time T , where T is called the time delay function. This escape process may be seen as a kind of instability and T can be seen as lifetime. In comparison to the first case, the asymptotic flatness of the potential is not necessary. When the potential is not bounded from below at spatial infinity, the escape process really means instability.

In this case, as we will see later, a fractal structure appears in the space of initial conditions for which remain in the scattering region. The singularities in the time delay function T form a Cantor-like set. This fractal is intrinsic to the escape process and different from the long-time behavior case.

We will consider the setup for the second one in a four-hill potential model in Sec. 3 and the BFSS matrix model in Sec 4.

3 Chaotic scattering in a four-hill potential model

We will here focus upon a prototypical model with a four-hill potential. We calculate the time delay function and present the associated fractal structure.

3.1 Four-hill potential model

Let us consider the Hamiltonian with a four-hill potential given by

$$H = \frac{p_x^2}{2} + \frac{p_y^2}{2} + x^2 y^2 \exp(-x^2 - y^2), \quad (3.1)$$

where the dynamical variables are $x(t)$ and $y(t)$, and the conjugate momenta are $p_x(t)$ and $p_y(t)$, respectively. The four-hill potential is flat for $|x|, |y| \gg 1$ and has peaks at $(x, y) = (\pm 1, \pm 1)$. The shape of this potential is depicted in Fig. 1. The chaotic region B is defined by $|x| < 2$ and $|y| < 2$ between the four hills as depicted in Fig. 2. Since the potential is asymptotically flat, chaotic scattering can be studied in both manners introduced above. Hereafter, we will follow the second manner (decay) because this is close to the analysis of the BFSS matrix model in Sec. 4.

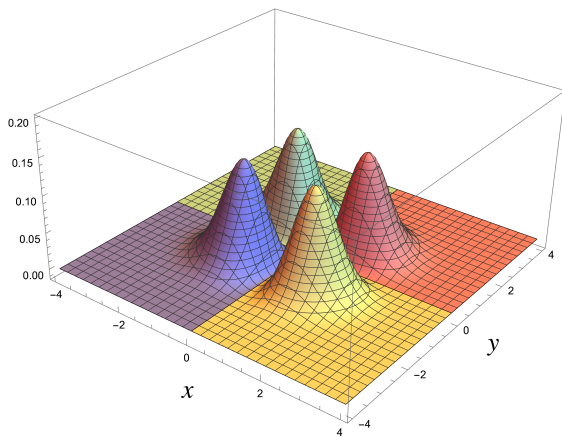


Figure 1: The shape of the four-hill potential.

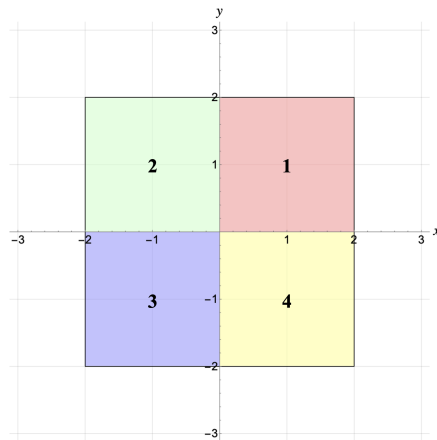


Figure 2: The chaotic region B . The region B is divided into the four regions.

3.2 Self-similarity in the initial points

Let us consider the (y, p_y) -plane of the initial conditions with $x = 0$, $p_x > 0$ and the energy $E = 0.001$ for which trajectories remain in the chaotic region B at a certain time t . The planes for $t = 70$, 100 and 150 are depicted in Fig. 3. Remarkably, one can see a

self-similarity of gaps in these figures. Figure 3 (a) illustrates the initial conditions for y and p_y for which the trajectories remain in the chaotic region B at $t = 70$. The figure on the right is a magnification of a part of the figure on the left. Similarly, Figures 3 (b) and (c) illustrate the initial conditions for which the trajectories remain in the chaotic region B at $t = 100$ and $t = 150$, respectively. The density decreases over time because more trajectories escape from the chaotic region B . Notice in the magnified figures on the right that there is a self-similar structure. At a fixed time t , smaller structures appear as one area is magnified. The self-similar structure becomes more and more prominent over time. This is nothing but the *fractal* structure associated with the chaotic scattering.

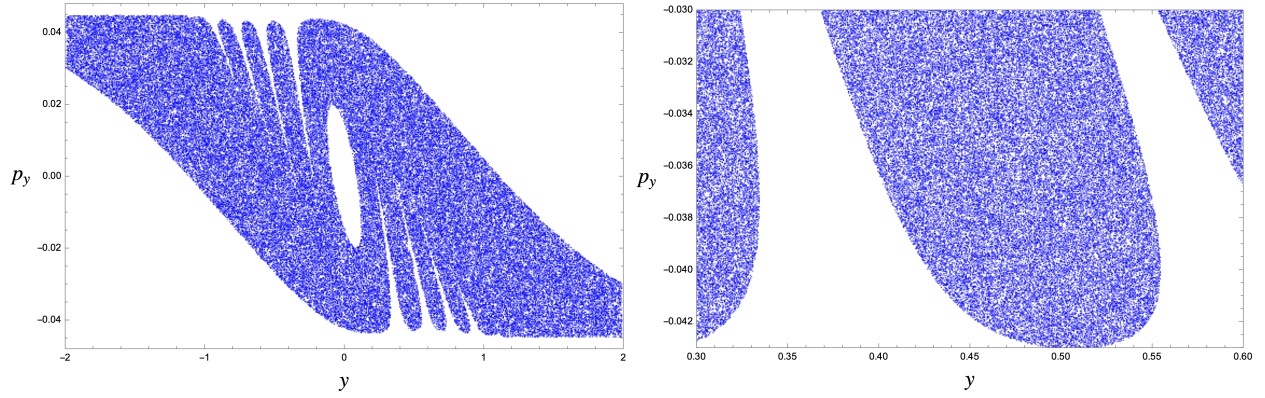
Symbolic dynamics

A traditional way to interpret a fractal structure behind chaos is to figure out the associated *symbolic dynamics*. A symbolic dynamics is generated by the following manner. Let us first divide the chaotic region B into four regions separated by the x and y axes, and each region is labelled by 1, 2, 3 and 4 denoted in Fig. 2. Regions 1, 2, 3 and 4 are colored by red, green, blue and yellow, respectively. Given a trajectory of a particle, one can trace it and record the labels when the particle enters into another region until it leaves the region B . The trajectory is then represented by a sequence of the labels such as $1 \rightarrow 2 \rightarrow 1 \rightarrow 4 \rightarrow 3 \dots$ (12143... for short).

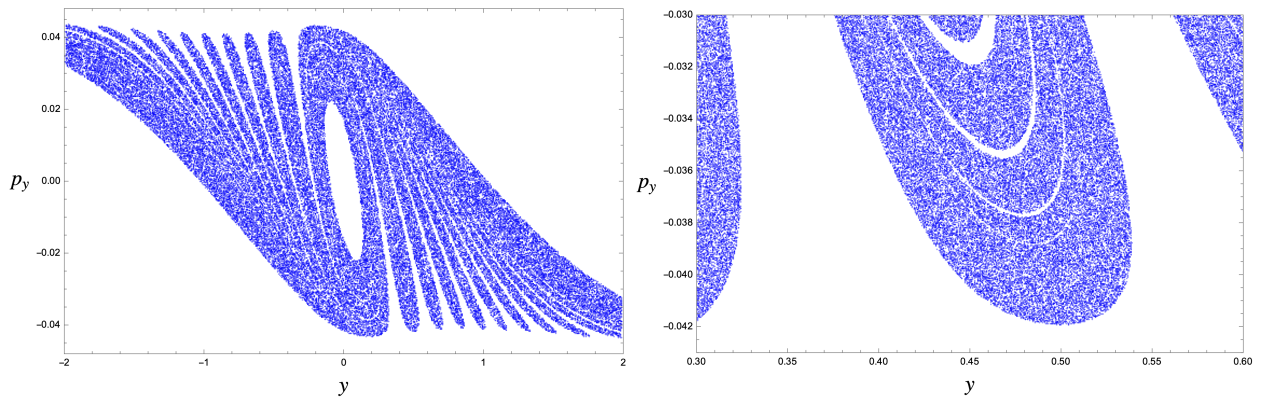
Consider a trajectory starting from a region, say 1. Depending on the initial condition, the particle can return to the region 1 through 121, 12321, 141 and so on. However, one can notice that there are also trajectories where the particle escapes between the hills. When plotting the initial points on the Poincaré section which remain in B , these escaping trajectories appear as gaps. Once the particle comes back to the region 1, the same procedure is repeated for infinite times. The Poincaré map for this system is thus given by a Smale horseshoe map, which is defined as infinite iterations of a map f from the (y, p_y) -plane into itself with stretching and folding.

The horseshoe construction indicates that the number of symbolic dynamics grows exponentially. It is the origin of infinitely self-similar structure, fractal. Indeed, the number of distinct trajectories is uncountable. This property distinguishes transient chaos from the other erratic behaviors.

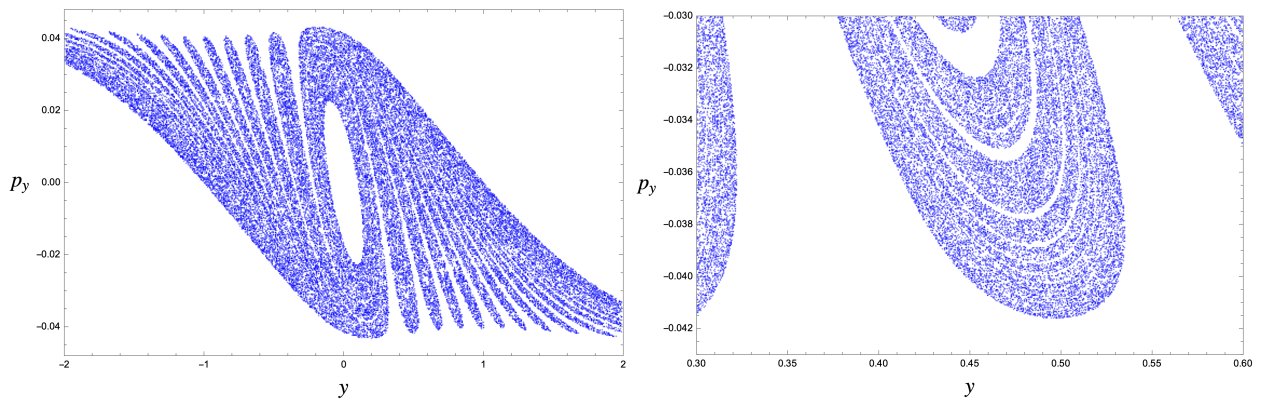
The horseshoe interpretation is valid for both chaos in a bounded space and transient chaos. In the latter case, although almost all trajectories are escaping, specific trajectories still remain in B after infinite time. The simplest case is with the initial condition $x = y > 0$



(a) The initial points which remain at $t = 70$



(b) The initial points which remain at $t = 100$



(c) The initial points which remain at $t = 150$

Figure 3: The initial conditions which remain in the chaotic region B . The other parameters are set to $x = 0$, $p_x > 0$ and $E = 0.001$. The figure on the right is an enlargement of the area of $0.3 < y < 0.6$ and $-0.043 < p_y < -0.03$ in the figure on the left.

and $p_x = p_y < 0$. In this case, the symbolic dynamics is described by $131313\dots$, and never ends.

3.3 Time delay function

Another feature of chaotic scattering can be seen in the behavior of the time delay function T . Figure 4 shows the time T to escape from the chaotic region B with respect to the initial condition. The initial condition is distributed for $x = 0$ in B , with $p_y = -0.03$ and $E = 0.001$. Namely, only y is an argument of T . The singular points corresponds to long-lived trajectories. The smooth intervals correspond to the gaps in Fig. 3. The figure on the right is a zoom-up of an area of the figure on the left. Even after magnifying the area, similar structure of smooth intervals appear. This self-similarity continues infinitely. Thus one can say that the singular points form a Cantor-like set² $\mathcal{C} \subset [-2, 2]$ though it is quite difficult to identify the dynamical map for this set concretely. In fact, the fractal dimension d (or box-counting dimension) of this set d ($0 < d < 1$) can be estimated as we will discuss below.

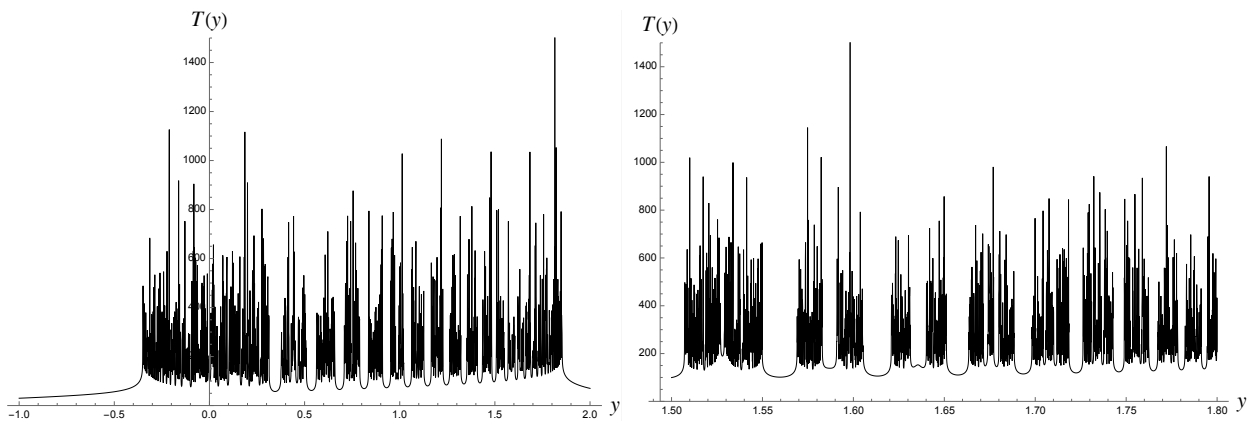


Figure 4: The escape time T with the initial condition $x = 0$, $p_y = -0.03$ and $E = 0.001$. The right figure zooms in on the area of $1.5 < y < 1.8$ in the left figure.

In the following, let us estimate the fractal dimension of \mathcal{C} by means of the *uncertainty fraction* $f(\epsilon)$. Choosing a random point $x_0 \in [-2, 2]$, we say that x_0 is ϵ -uncertain if $|T(x_0 + \epsilon) - T(x_0)| > h$, where the positive number h is taken to be a typical escaping time, say 100. We take random reference points x_0 , and tell whether these are ϵ -uncertain or not.

²In the analogy with the Cantor ternary set, the smooth interval corresponds to the middle 1/3 interval to be truncated.

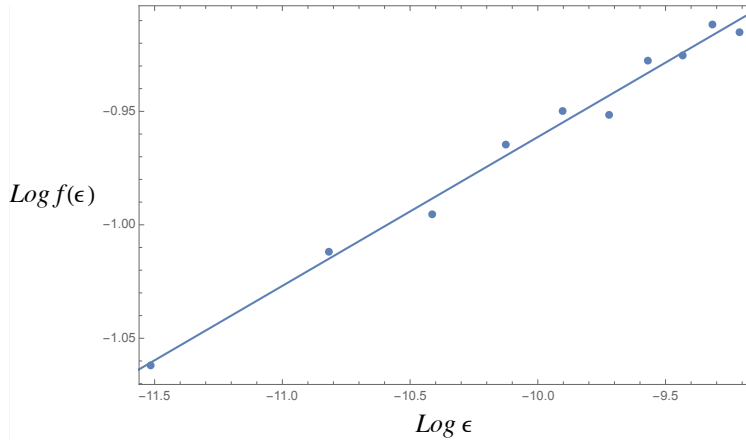


Figure 5: The uncertain fraction with $h = 50$. The axes are given by the natural logarithms.

The uncertainty fraction $f(\epsilon)$ is obtained by dividing the number of uncertain points by the total number of chosen random points. We then define the uncertainty dimension by

$$d_u := 1 - \lim_{\epsilon \rightarrow +0} \frac{\log f(\epsilon)}{\log \epsilon}. \quad (3.2)$$

The box-counting dimension d_{box} is often adopted as a fractal dimension. In typical dynamical systems, d_{box} is shown to be equal to the uncertainty dimension d_u [13]. To understand the relation between these dimensions, suppose $f(\epsilon)$ equals to the probability such that a singularity is included in $x \in [x_0, x_0 + \epsilon]$. Under this assumption, the box-counting dimension is given by

$$d_{\text{box}} = \lim_{\epsilon \rightarrow +0} \frac{\log(4/\epsilon \cdot f(\epsilon))}{\log(4/\epsilon)} = 1 + \lim_{\epsilon \rightarrow +0} \frac{\log f(\epsilon)}{\log(4/\epsilon)} = d_u. \quad (3.3)$$

In this paper, we refer to the uncertain dimension d_u as the fractal dimension d , i.e.,

$$d = d_u. \quad (3.4)$$

The uncertain dimension can be obtained by fitting the plot of $\log f(\epsilon)$ versus $\log \epsilon$ as shown in Fig. 5. For each value of ϵ , 10^4 points are taken as random reference points x_0 . From this figure, one can read off the following relation:

$$\log f(\epsilon) = 0.066 \log \epsilon - 0.31. \quad (3.5)$$

Thus the fractal dimension d for this initial condition is given by $d = 0.93$.

4 Chaotic instability in the BFSS matrix model

In this section, we shall discuss chaotic scattering in the BFSS matrix model. The BFSS matrix model is a one-dimensional $U(N)$ gauge theory with adjoint matters. The bosonic part of the classical action is given by

$$S = \int dt \operatorname{tr} \left(\frac{1}{2} \sum_{r=1}^9 (DX^r)^2 + \frac{1}{4} \sum_{r,s=1}^9 [X^r, X^s]^2 \right), \quad (4.1)$$

$$DX^r := \frac{d}{dt} X^r - i[A, X^r], \quad (4.2)$$

where $X^r(\tau)$ are $N \times N$ hermitian matrix-valued variables. The equation of motion for a gauge field A leads to the Gauss-law constraint

$$0 = \sum_{r=1}^9 [X^r, DX^r]. \quad (4.3)$$

By taking a variation with respect to X^r , the equations of motion are obtained as

$$0 = \frac{d^2}{dt^2} X^r + \sum_{s=1}^9 [X^s, [X^s, X^r]], \quad (4.4)$$

where we have taken a static gauge $A = 0$ and hereafter will work in this gauge. Note that the classical action (4.1) has flat directions along the Abelian subalgebra. Since this property allows unbounded motions, one may discuss chaotic scattering in this system. In the following, we consider the $N = 2$ case for simplicity.

Next, let us reduce the equations of motion by supposing a specific ansatz:

$$\begin{aligned} X^1(t) &= x(t) \frac{\sigma^1}{2}, & X^2(t) &= y(t) \frac{\sigma^2}{2}, & X^3(t) &= z(t) \frac{\sigma^3}{2}, \\ X^s(t) &= 0 & (s = 4, \dots, 9). \end{aligned} \quad (4.5)$$

Here σ^1 , σ^2 and σ^3 are the Pauli matrices and $x(t)$, $y(t)$ and $z(t)$ are functions to be determined. The Gauss Law constraint (4.3) is automatically satisfied under the ansatz (4.5). In light of [15], this configuration can be interpreted as a pulsating membrane. The equations of motion (4.4) are then reduced to

$$\begin{aligned} 0 &= \frac{d^2}{d\tau^2} x(t) + x(t)(y(t)^2 + z(t)^2), \\ 0 &= \frac{d^2}{d\tau^2} y(t) + y(t)(z(t)^2 + x(t)^2), \\ 0 &= \frac{d^2}{d\tau^2} z(t) + z(t)(x(t)^2 + y(t)^2). \end{aligned} \quad (4.6)$$

Here, let us impose a further constraint $z(t) = 0$. This does not spoil down the Gauss law constraint (4.3). From the point of view of membrane dynamics, this constraint means that the diameter for the X^3 -direction is set to zero. Under this constraint, the equations of motion (4.6) are further reduced to

$$0 = \frac{d^2}{dt^2}x(t) + x(t)y(t)^2, \quad 0 = \frac{d^2}{dt^2}y(t) + x(t)^2y(t). \quad (4.7)$$

Note that these equations of motion are derived also from the Hamiltonian

$$H = \frac{p_x^2}{2} + \frac{p_y^2}{2} + \frac{x^2y^2}{2}. \quad (4.8)$$

This system was also considered in [4,6]. Note here that this system (4.8) can also be derived from a four-dimensional classical Yang-Mills theories as shown in [4]. Hence the results we will obtain below hold for the four-dimensional Yang-Mills theory beyond the BFSS matrix model.

The potential in (4.8) is zero on the x - and y -axes (see Fig. 6) and hence the diameter in either direction can be expanded to any width in a finite amount of time. Therefore, one may consider the membrane decay as a process of chaotic scattering and discuss the associated fractal structure as in the four-hill potential case.

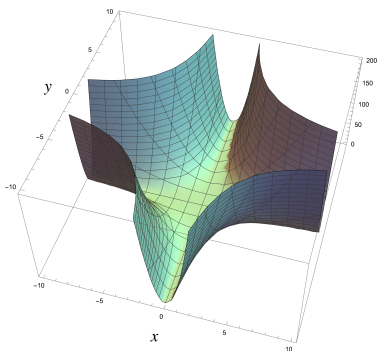


Figure 6: The shape of the potential $x^2y^2/2$.

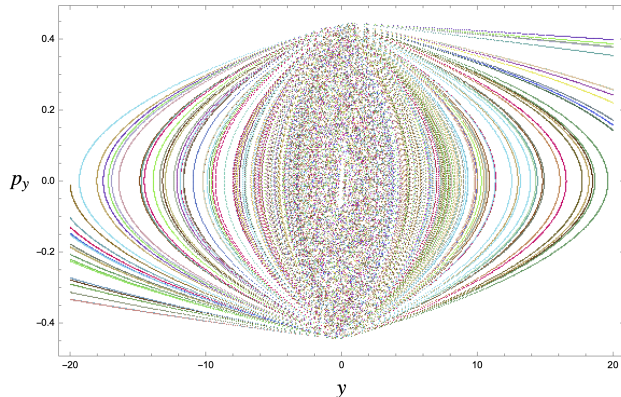


Figure 7: Poincaré sections for $E = 0.1$. Each color represents a different trajectory.

Following the standard method, we can compute Poincaré sections as shown in Fig. 7. Calculations are stopped if orbits reach $|y| = 20$ so as to avoid numerical errors. When $E = 0.1$, motions are no longer chaotic once the point leaves the region around $|y| \leq 4$. Therefore, we take the chaotic region B as the box $|x| < 5, |y| < 5$. Outside the region B , points go far away along the “paths” for $x = 0$ or $y = 0$ while oscillating in the “valleys”³.

³For an alternative approach to define the lifetime, see an intriguing work [16].

We can calculate remaining trajectories and time delay function by the same procedure as in Sec. 3. When starting from the initial condition such that $x = 0$, $E = 0.1$ and $-5 < y < 5$, some of motions escape B at $t = 70$. Figure 8 shows the remaining initial conditions in the (y, p_y) -plane.

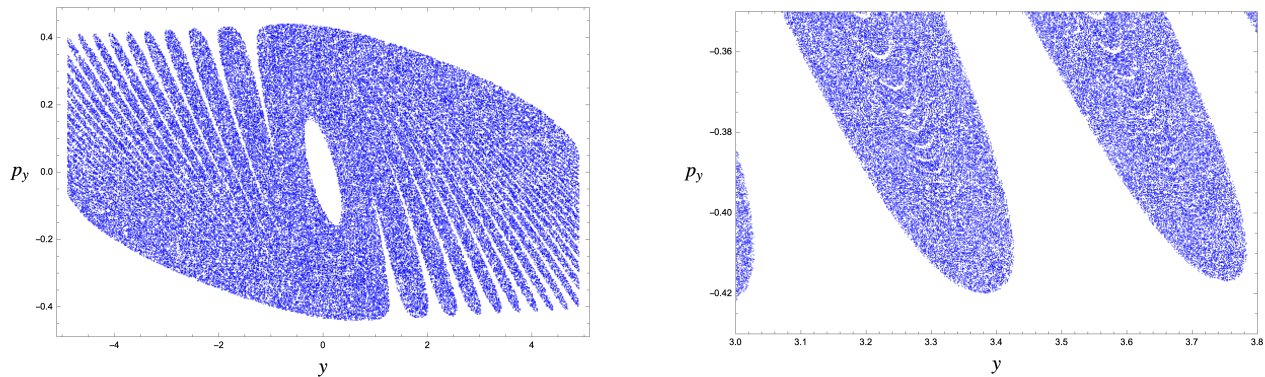


Figure 8: Initial conditions which remain in B at $t = 70$. The figure on the right is a zoomed-in view of the area of $3.0 < y < 3.8$, $-0.043 < p_y < -0.35$ in the figure on the left.

Then, we have computed the time delay function for the initial condition $x = 0$ and $p_y = 0.3$ (as shown in Fig. 9). There are singularities and smooth intervals as in the four-hill potential case. By zooming up to a part of the graph, a self-similar structure can be observed. The singularities form a Cantor-like set again and its fractal dimension can be estimated by using the uncertain fraction.

The uncertain dimension is computed based on Fig. 10, where we took 10^4 reference points x_0 . As a result, the uncertain fraction is fitted as

$$\log f(\epsilon) = 0.050 \log \epsilon - 0.42, \quad (4.9)$$

and thus the fractal dimension is given by

$$d = 0.95. \quad (4.10)$$

After all, the singularities of the time delay function under the ansatz (4.5) indeed exhibit a fractal structure. This indicates that the membrane instability is identified with chaotic instability.

For the bosonic matrix model, quantum corrections lift up all of the flat directions and bosonic membranes are stable. But in the case of supermembranes, the quantum corrections vanishes due to the presence of supersymmetries. Hence the supermembrane is unstable in the same manner as in the case of bosonic membranes at classical level. Thus, the chaotic instability discussed above is common to the supermembrane at quantum level.

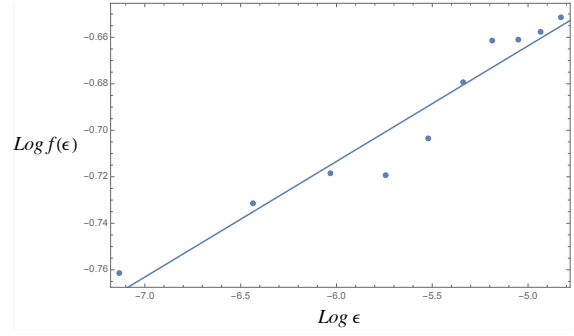
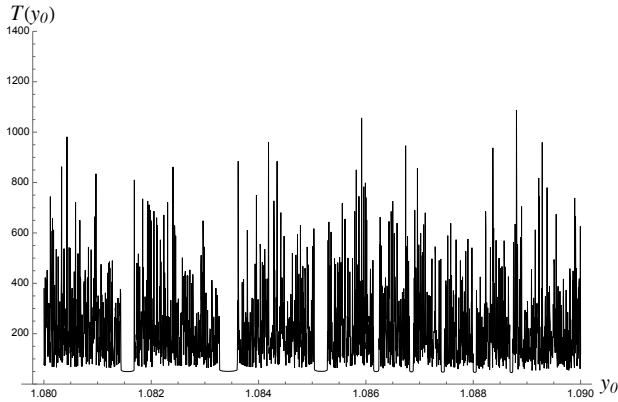
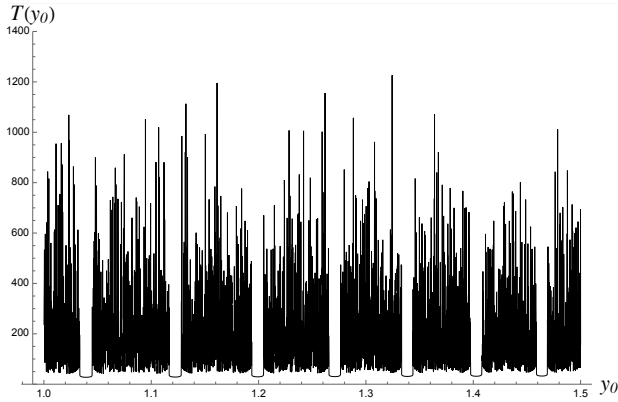
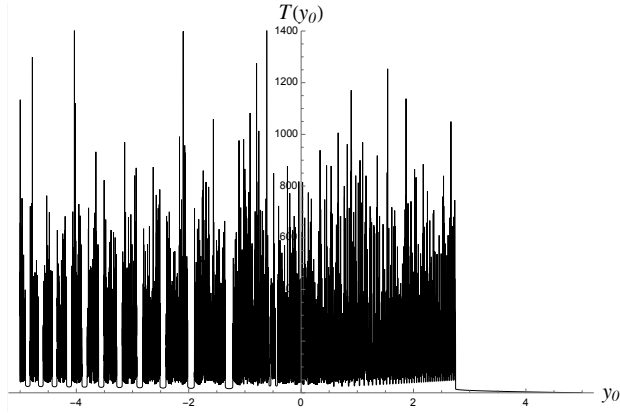


Figure 10: The uncertain fraction with $h = 100$. The axes are given by the natural logarithms.

Figure 9: Time delay function for $x = 0$, $p_y = 0.3$, $E = 0.1$. Here y_0 is an initial value of y . The second is a zoom-up of the range $1.0 < y_0 < 1.5$. The third is a zoom-up of the range $1.08 < y_0 < 1.09$.

5 Conclusion and Discussion

We have considered chaotic scattering in the BFSS matrix model. The membrane instability associated with the flat directions in the potential is identified as chaotic scattering. For a reduced system, we have shown a fractal structure in the space of initial conditions for which a certain type of membrane moves in the chaotic region. In addition, we have shown that the singularities in the time delay function form a Cantor-like set and estimated its fractal dimension. Thus a fractal structure in the membrane decay process has been revealed.

Our analysis here has been carried out with fixed coupling constant and a certain value of the energy. The strength of transient chaos varies depending on values of the coupling constant and energy. Elucidating the dependence of the fractal dimension on the coupling constant and energy is an interesting problem (For a similar direction, see a recent interesting work [17]). For this issue, we will report in another place in the near future.

There are other questions. We have discussed here chaotic scattering at classical level. It is interesting to take quantum corrections into account. In the bosonic matrix model, all of the flat directions are lifted up by quantum corrections. However, in the supermembrane case, the quantum corrections are cancelled out by supersymmetries and the instability survives. The ground-state wave function of a supermembrane is constructed in [18]. It is interesting to study the relation between this wave function and the fractal structure revealed in this paper. In general, the self-similar structure in fractal is truncated at the Planck scale at quantum level. It is significant to figure out this truncation mechanism.

It is also interesting to look for applications of the fractal structure in the context of the gauge/gravity correspondence. It may be related to graviton scattering in eleven-dimensional supergravity. The results obtained here is also common to the four-dimensional classical Yang-Mills theory. Therefore, the corresponding phenomenon should exist on AdS_5 , though we have no idea what it is indeed. We hope that our fractal result will shed light on a new aspect of the gauge/gravity correspondence.

Acknowledgments

We are very grateful to Koji Hashimoto for useful comments and discussions. The work of O.F. was supported by Grant-in-Aid for JSPS Fellows No. 21J22806. The work of K.Y. was supported by JSPS Grant-in-Aid for Scientific Research (B) No. 18H01214.

References

- [1] V. Rosenhaus, “Chaos in the Quantum Field Theory S-Matrix,” *Phys. Rev. Lett.* **127** (2021) 021601 [arXiv:2003.07381 [hep-th]].
- [2] D. J. Gross and V. Rosenhaus, “Chaotic scattering of highly excited strings,” *JHEP* **05** (2021) 048 [arXiv:2103.15301 [hep-th]].
- [3] V. Rosenhaus, “Chaos in a many-string scattering amplitude,” [arXiv:2112.10269 [hep-th]].
- [4] S. G. Matinyan, G. K. Savvidy and N. G. Ter-Arutunian Savvidy, “CLASSICAL YANG-MILLS MECHANICS. NONLINEAR COLOR OSCILLATIONS,” *Sov. Phys. JETP* **53** (1981) 421-425
- [5] T. Banks, W. Fischler, S. H. Shenker and L. Susskind, “M theory as a matrix model: A Conjecture,” *Phys. Rev. D* **55** (1997) 5112-5128 [arXiv:hep-th/9610043 [hep-th]].
- [6] I. Y. Aref’eva, P. B. Medvedev, O. A. Rytchkov and I. V. Volovich, “Chaos in M(atrix) theory,” *Chaos Solitons Fractals* **10** (1999) 213-223 [arXiv:hep-th/9710032 [hep-th]].
- [7] D. E. Berenstein, J. M. Maldacena and H. S. Nastase, “Strings in flat space and pp waves from N=4 superYang-Mills,” *JHEP* **04** (2002) 013 [arXiv:hep-th/0202021 [hep-th]].
- [8] Y. Asano, D. Kawai and K. Yoshida, “Chaos in the BMN matrix model,” *JHEP* **06** (2015), 191 [arXiv:1503.04594 [hep-th]].
- [9] B. de Wit, J. Hoppe and H. Nicolai, “On the Quantum Mechanics of Supermembranes,” *Nucl. Phys. B* **305** (1988) 545.
- [10] B. de Wit, M. Lüscher and H. Nicolai, “The Supermembrane is Unstable,” *Nucl. Phys. B* **320** (1989) 135.
- [11] J. M. Seoane, and M. AF. Sanjuán. “New developments in classical chaotic scattering.” *Reports on Progress in Physics* 76.1 (2012): 016001.
- [12] H. C. Lai, T. Tél, “Transient chaos: complex dynamics on finite time scales.” Vol. 173. Springer Science & Business Media, 2011.

- [13] H. E. Nusse, J. A. Yorke, “The equality of fractal dimension and uncertainty dimension for certain dynamical systems,” *Commun. Math. Phys.* **150** (1992) 1-21.
- [14] G. H. Hsu, E. Ott, and C. Grebogi, “Strange saddles and the dimensions of their invariant-manifolds,” *Phys. Lett. A* **127** (1988) 199-204.
- [15] D. N. Kabat and W. Taylor, “Spherical membranes in matrix theory,” *Adv. Theor. Math. Phys.* **2** (1998) 181-206 [arXiv:hep-th/9711078 [hep-th]].
- [16] D. Berenstein and Y. Guan, “Improved semiclassical model for real-time evaporation of matrix black holes,” *Int. J. Mod. Phys. A* **36** (2021) no.29, 2150219 [arXiv:2105.04577 [hep-th]].
- [17] K. Hashimoto, K. Murata, N. Tanahashi and R. Watanabe, “A bound on energy dependence of chaos,” [arXiv:2112.11163 [hep-th]].
- [18] P. Yi, “Witten Index and Threshold Bound States of D-Branes,” *Nucl. Phys.* **B505** (1997) 307, hep-th/9704098.
S. Sethi and M. Stern, “D-Brane Bound States Redux,” *Commun. Math. Phys.* **194** (1998) 675, hep-th/9705046.